MODE SHAPES VARIATION OF A COMPOSITE BEAM WITH PIEZOELECTRIC PATCHES

FOTIOS GEORGIADES, JAROSŁAW LATALSKI, JERZY WARMIŃSKI

Lublin University of Technology

Summary

In this paper the modal shapes of a light, thin laminate beam with active elements were evaluated. Cases with one or two Macro Fiber Composite (MFC) active elements adhered onto a glass-epoxy cantilever beam were analyzed. The systems under consideration were modeled in ABAQUS finite element software to derive mode shapes numerically. Next, the modes were compared to each other to estimate the influence of PZT patches. First 20 modes of natural vibrations were examined including bending, torsion and axial ones. The comparisons of mode shapes were performed according to Modal Assurance Criterion (MAC) analysis. The examination of changes of mode shapes of the original beam with placement of active elements is the starting point in prior of optimal placements of PZTs with final goal the control of dynamics of helicopter blades.

INTRODUCTION

Composite laminate materials are widespread in the fields of aircraft and spacecraft constructions and are continuously increasing within other fields of application. However, high demands to the modern structures tend to combine these composite materials with other ones. One of the most promising perspectives is embedding of piezoelectric actuators because of their advantages of fast response, no magnetic fields, no wear etc. This smart structures technology has the potential to significantly influence aerospace, wind energy etc. industries in e.g. vibration control (induce vibration, vibration mitigation, energy harvesting, adaptronics etc.) and also in structural health monitoring tasks.

The aim of the current study was to examine numerically the mode shapes of a thin multilayer composite cantilever beam. At the second stage of research the effects related to adding PZT patches to the master beam were investigated. The mode shapes for modified systems were compared to the modes of the initial design by means of MAC analysis. Four distinct PZT configurations were checked – one or two symmetric actuators at the clamping or alternatively, at the free end. An exemplary configuration with one patch is shown in Figure 1 (dimensions in mm).
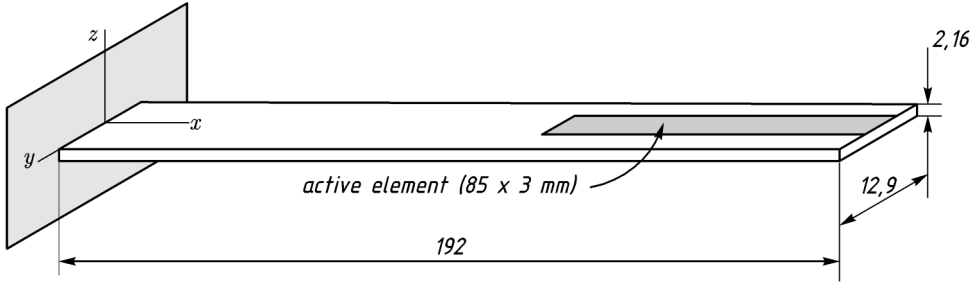
Figure 1. Composite beam under consideration; one PZT element at the free end

ANALYTICAL MODEL

The system under consideration was described according to Euler-Bernoulli beam theory, where rotary inertia terms were neglected [3, 4, 6]:

$$\frac{\partial N_{xx}}{\partial x} = I_0 \frac{\partial^2 u}{\partial t^2}$$

$$\frac{\partial^2 M_{zz}}{\partial x^2} = I_0 \frac{\partial^2 v}{\partial t^2}$$

$$\frac{\partial^2 M_{yy}}{\partial x^2} = I_0 \frac{\partial^2 w}{\partial t^2}$$

$$\frac{\partial M_{xx}}{\partial x} = J_{xx} \frac{\partial^2 \varphi}{\partial t^2}$$

where u, v, w were displacements in x, y, and z directions respectively and the rotation with respect to x-axis,
N_{xx} in-plane force resultants and M_{xx}, M_{yy}, M_{zz} the moment resultants with respect to x, y, and z axis respectively,
$I_0 = \int_{h_{min}}^{h_{max}} \rho dz$ – mass inertia term and $J_{xx} = \int_{h_{min}}^{h_{max}} \rho \left(y^2 + z^2 \right) dy dz$.

The boundary conditions for the above equations were defined at free end (no shear force and bending moment):

$$\frac{\partial M_{xx}(l,t)}{\partial x} = 0, \ M_{xx}(l,t) = 0, \ \frac{\partial M_{yy}(l,t)}{\partial x} = 0, \ M_{yy}(l,t) = 0$$

$$\frac{\partial M_{zz}(l,t)}{\partial x} = 0, \ M_{zz}(l,t) = 0$$

and at clamping (no displacement and rotation):

$$u(0,t) = 0, \ \frac{du(0,t)}{dx} = 0, \ v(0,t) = 0, \ \frac{dv(0,t)}{dx} = 0, \ w(0,t) = 0, \ \frac{dw(0,t)}{dx} = 0$$

$$\varphi(0,t) = 0, \ \frac{d\varphi(0,t)}{dx} = 0$$

NUMERICAL MODEL

The master beam was made of unidirectional glass fibers tape and epoxy Prime 20 (Sicomin 8100 + hardener 8824, fibers ratio 50±2%, E_f = 69 000 MPa, E_m = 3 500 MPa, v_f = 0.2, v_m = 0.37, ρ_f = 2.56 g/cm^3, ρ_m = 1.2 g/cm^3 – all data by manufacturer of a specimen). Based on this the equivalent material properties of a single lamina layer were calculated by rule of mixtures [5]: averaged density ρ_{av} = 1.85 g/cm^3, Young modulus along fibers E_1 = 36 250 MPa, transversal Young modulus E_2 = 6662 MPa, shear moduli G_{12} = G_{13} = G_{23} = 2446 MPa and Poisson's ratio v_{12} = 0.285. The subsequent layers of the composite were set in the following order: 0°/90°/+45°/-45°/+45°/90°/0° (according to Ox axis pointing side edgewise).

The MFC patch material data used in the analysis was sourced from Smart Systems Inc. For the simulation the following electric and elastic properties were used: isotropic ferroelectric material with constant permittivity ξ = 8 · 10^9 F/m and mean value of piezoelectric coefficient d_{33}= 59 ·10^{-9} m/V; elastic orthotropic material having Young moduli E_1 = E_2 = 15 857 MPa, E_3 = 30 336 MPa, shear moduli G_{12} = G_{13} = G_{23} = 5 515 MPa and Poisson ratios v_{12} = v_{13} = v_{23} = 0.30.

The numerical model of a beam was developed in ABAQUS software. Specimen was defined as a lamina type; and this approach enabled modeling the composite as a set of orthotropic layers in plane-stress state by a Layup-Ply technique [1]. For beam meshing shell elements S4R were used – i.e. linear ones with reduced integration. The actuator was defined by means of second order continuum elements – C3D20RE ones. The final FEM model consisted of 1517/1534 elements and 1873/2085 nodes in total (depending on the number of PZT patches).

The composite material data, electrical properties of PZTs and specimen dimensions used for the numerical tests correspond to the actual beam installed in Laboratory of Dynamics and Strength of Materials at Lublin University of Technology to be used later for experimental validation.

RESULTS

Within the framework of research program first 20 modes of natural vibrations were examined. These included bending, torsion and axial ones as reported in Table 1. The analysis was run for five different cases: composite beam without any active elements, one active element at the free end and next at the clamping and finally, two PZTs at free end and two PZTs at clamping.

Table 1. Modes of natural vibrations of the composite beam under consideration (in bold the 'mixed' modes), superscripts "c" and "f" denote the case with actuator(s) at clamped and free end respectively

Mode shape	Beam without PZT/PZTs			
Bending xy plane	2, 6, 11, 17			
Bending xz plane	1, 3, 5, 7, 9, 12, 15, 18, 20			
Torsion	4, 8, 10, 13, 16, 19			
Axial	14			
Mode shape	1-PZT^f	2-PZT^f	1-PZT^c	2-PZT^c
Bending xy plane	2, 6, **10, 11, 16, 17**	2, 6, 10, 16	2, 6, **10, 11, 16, 17**	2, 6, 10, 16
Bending xz plane	1, 3, 5, 7, 9, 12, 15, 18, 20	1, 3, 5, 7, 9, 12, 15, 18, 20	1, 3, 5, 7, 9, 12, 15, 18, 20	1, 3, 5, 7, 9, 12, 15, 18, 20
Torsion	4, 8, **10, 11**, 14, **16, 17**	4, 8, 11, 14, 17, 19	4, 8, **10, 11**, 13, **16, 17**, 19	4, 8, 11, 14, 17, 19
Axial	13	13	14	13

For each of the modes the corresponding frequency of natural vibration was calculated. Results for the discussed cases are presented in Table 2. It was shown, that the shift in natural frequencies is more prominent for lower modes; especially for the case of torsion and for bending in the plane of lower stiffness.

Table 2. Comparison of natural frequencies of analyzed systems; superscript "c" denotes the case with actuator(s) at clamped end, superscript "f" denotes the case with actuator(s) at free end

	1	2	3	4	5	6	7	8	9	10
0 PZT	35.48	170.21	221.94	532.29	619.69	1042.74	1209.47	1607.75	1989.17	2715.06
1 PZTc	37.73	170.15	228.90	563.63	635.10	1022.55	1232.93	1642.59	2037.79	2740.66
1 PZTf	33.55	160.62	221.27	534.19	625.15	1014.30	1225.40	1675.37	2041.40	2739.27
2 PZTc	39.99	170.09	234.86	588.24	651.50	1003.73	1255.59	1669.65	2084.50	2674.75
2 PZTf	31.91	152.50	220.46	533.74	631.92	988.43	1240.10	1725.00	2091.23	2678.46

	11	12	13	14	15	16	17	18	19	20
0 PZT	2822.39	2953.38	3873.55	3955.32	4095.54	5100.37	5288.94	5407.68	6408.99	6881.82
1 PZTc	2796.26	3013.87	3980.84	4006.48	4177.73	5165.97	5220.38	5510.26	6572.24	6992.87
1 PZTf	2800.10	3023.93	3785.21	3999.76	4183.66	5172.28	5256.98	5515.80	6584.17	7005.49
2 PZTc	2849.05	3079.07	4055.56	4068.55	4253.81	5061.58	5301.40	5619.22	6699.88	7097.54
2 PZTf	2857.90	3103.50	3636.89	4088.01	4270.59	5072.88	5379.62	5634.68	6709.93	7125.84

For the description of calculated mode shapes 71 nodes along the length and width of a sample structure were selected (see Figure 2). Translational and rotational degrees of freedom in each node were recorded resulting in configuration space vector having 426 elements in total.
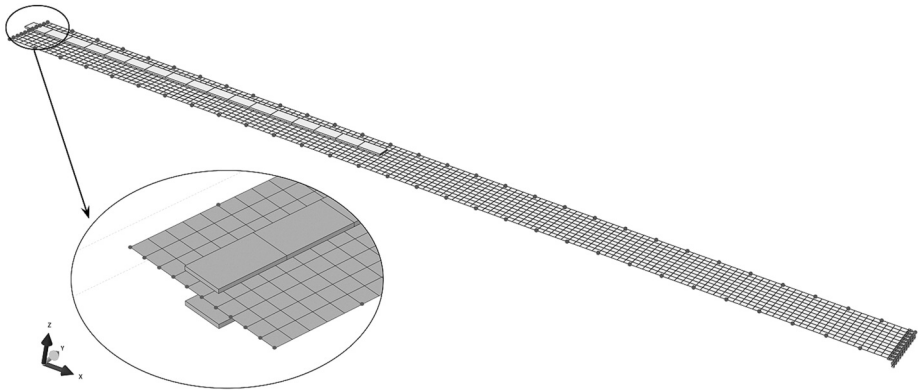

Figure 2. Nodes to describe the beam mode shape

Mode shapes of the beam with PZT patch/patches were compared to the shape of the reference specimen (i.e. the same beam without any PZTs). For quantifying the degree of compatibility between modes Modal Assurance Criterion (MAC, also referred to as Mode Shape Correlation Coefficient) was applied. This provided a measure of the least-squares deviation of the points from the straight line correlation defined by:

$$MAC(A,B) = \frac{\left| \sum_{j=1}^{n} \varphi_{Aj} \varphi_{Bj} \right|^2}{\left| \sum_{j=1}^{n} \varphi_{Aj} \varphi_{Aj}^* \right| \left| \sum_{j=1}^{n} \varphi_{Bj} \varphi_{Bj}^* \right|}$$

where φ_A, φ_B – configuration vectors to be compared and n – their dimension (* denotes the transpose). According to the literature, it was assumed that MAC value in excess of 0.9 corresponded to well-correlated modes [2].

To estimate the influence of PZT on mode shapes four MAC tests were performed: the reference beam was compared to the system with one PZT (placed at free end or at clamping) and next to the system with 2 PZTs (placed symmetrically both at free end or both at clamping). Results of comparison tests are presented graphically in Figure 3. Next, four additional tests were run to evaluate the effects related to the change in number of PZTs used (beam with 1 PZT at free end vs system with 2 PZTs at free end and beam with 1 PZT at clamping vs system with 2 PZTs at clamping) or to the change of PZT/PZTs position (beam with 1 PZT at clamping vs beam with 1 PZT at free end and 2 PZTs at clamping vs 2 PZTs at free end). Results of these tests are presented graphically in Figure 4.
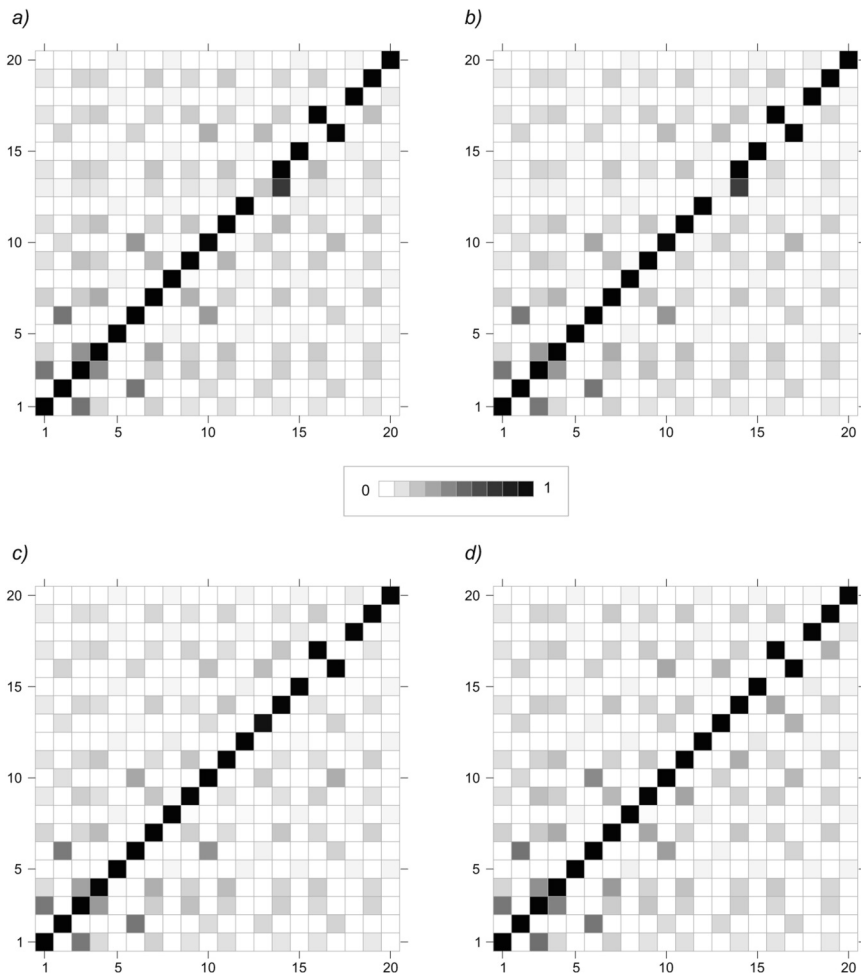

Figure 3. Graphical results of MAC analysis:
a) reference beam vs system with 1 PZT at free end,
b) reference beam vs system with 1 PZT at clamping,
c) reference beam vs system with 2 PZTs at free end,
d) reference beam vs system with 2 PZT at clamping

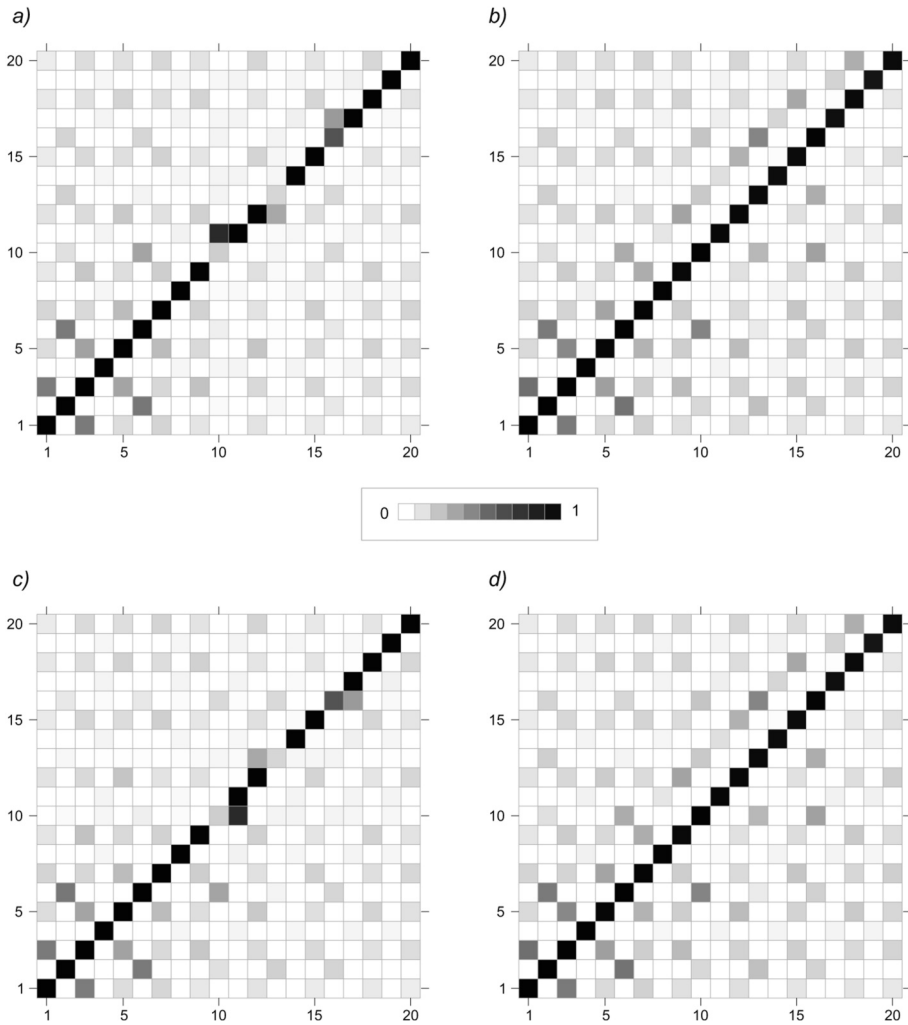Figure 4. Graphical results of MAC analysis cont.:
a) beam with 1 PZT at free end vs system with 2 PZTs at free end,
b) beam with 1 PZT at clamping vs system with 2 PZTs at clamping,
c) beam with 1 PZT at clamping vs system with 1 PZT at free end,
d) 2 PZTs at clamping vs 2 PZTs at free end

As a supplement to the above figure the accurate values of MAC diagonal – which is the comparison between the same mode shapes – are tabulated in Table 3.

Table 3. Diagonal of MAC analysis for the discussed cases; indices "c" and "f" denote the case with actuator(s) at clamped and free end. The cases where the mode agreement was not achieved are distinguished by bold typeface

	1	2	3	4	5	6	7	8	9	10
$0 - 1^f$	1.000	0.994	1.000	1.000	0.998	0.999	0.997	0.997	0.995	**0.773**
$0 - 1^c$	1.000	0.999	0.999	1.000	0.995	0.998	0.998	0.999	0.997	**0.557**
$0 - 2^f$	1.000	1.000	0.998	0.999	0.994	1.000	0.990	0.991	0.979	**0.000**
$0 - 2^c$	0.999	1.000	0.996	0.998	0.982	1.000	0.993	0.998	0.987	**0.000**
$1^f - 2^f$	1.000	0.994	1.000	1.000	0.999	0.999	0.998	0.998	0.994	***0.226***
$1^c - 2^c$	1.000	0.999	0.999	1.000	0.996	0.998	0.999	1.000	0.997	***0.435***
$2^f - 2^c$	0.998	1.000	0.990	0.996	0.959	0.999	0.970	0.981	0.935	0.990

	11	12	13	14	15	16	17	18	19	20
$0 - 1^f$	**0.003**	0.996	**0.053**	**0.000**	0.993	**0.397**	**0.002**	0.995	0.986	0.993
$0 - 1^c$	**0.001**	0.997	0.995	**0.013**	0.996	**0.537**	**0.003**	0.996	0.991	0.996
$0 - 2^f$	**0.000**	0.983	**0.000**	**0.000**	0.977	**0.000**	**0.000**	0.979	0.959	0.974
$0 - 2^c$	**0.000**	0.988	**0.000**	**0.000**	0.985	**0.000**	**0.000**	0.984	0.972	0.985
$1^f - 2^f$	0.995	0.996	***0.193***	0.995	0.994	***0.601***	0.993	0.995	0.992	0.994
$1^c - 2^c$	0.997	0.997	***0.000***	0.962	0.996	***0.459***	0.994	0.996	0.995	0.997
$2^f - 2^c$	0.956	0.948	0.931	0.920	0.928	0.984	0.900	0.930	0.868	0.924

CONCLUSIONS

– PZTs added to the reference beam resulted in values of natural frequencies to get shifted – see Table 2. This effect might be both of inertial type (decreasing frequency) and stiffening type (increasing frequency) as well. The observed frequency shifting is more prominent for lower modes; especially for the case of torsion and for bending in the plane of lower stiffness.
– There was no significant difference in mode shapes for placement of 2 PZTs at clamped end or at free end.
– Adding 2 PZTs there was a swap in frequencies of 10, 11, 13 and 14 modes, e.g. order of these bending and torsion modes got reversed.
– Placement of 1 PZT caused the system to be asymmetric. This resulted in modes 10, 11, 16, 17 to have been mixed motion between torsion and xy-bending.
– It is expected that significant differences to the reported ones might happen in cases with PZT exposed to voltage. The series of the appropriate tests will be run during further research.
– We intend to perform a series of similar laboratory tests and to compare the results to the outcomes of these numerical simulations.
– The mode shapes variation of the original beam with placement of PZT patches, is the starting point of our research for optimal position of PZT since as we showed in Table 1 there are structural changes of the mode shapes. As next steps will also be examined the effect of mode shapes variation of a rotating beam. Final goal of our research is a control of dynamics of helicopter blades with active elements.

REFERENCES

[1]   –: ABAQUS User's Manual (6.10), Dassault Systèmes, 2010.
[2]   Ewins D.J.: Modal Testing – Theory, Practice and Applications. Research Institute Press Ltd, Philadelphia 2000.
[3]   Kollar, P.L., Springer, G.S., Mechanics of Composite Structures, Cambridge, Cambridge University Press 2003.
[4]   Reddy J.N.: Mechanics of Laminated Composite Plates and Shells – Theory and Analysis. CRC Press, Boca Raton (FL) 2004.
[5]   Staab G.H.: Laminar Composites. Butterworth-Heinemann, Boston, 1999.
[6]   Nayfeh, A.H., Pai, P.F.: Linear and Nonlinear Structural Mechanics, John Wiley & Sons, Hoboken, New Jersey, 2004.

Fotios Georgiades, Jarosław Latalski, Jerzy Warmiński

POSTACIE DRGAŃ BELKI KOMPOZYTOWEJ Z ELEMENTAMI PIOZOELEKTRYCZNYMI

Streszczenie
W pracy przedstawiono wyniki analizy modalnej lekkiej, cienkiej belki kompozytowej, jednostronnie utwierdzonej, z osadzonymi elementami aktywnymi. Na wstępie przeanalizowano belkę wzorcową – tj. wykonaną z laminatu żywiczno-szklanego bez elementów aktywnych. Następnie zbadano tę samą belkę z dodanym jednym, a w dalszej kolejności także z dwoma kompozytowymi elementami aktywnymi typu MFC (Macro Fiber Composite). Częstości i postacie drgań własnych badanych układów określono numerycznie za pomocą metody elementów skończonych – wykorzystano w tym celu oprogramowanie ABAQUS. Wyznaczono i zbadano 20 pierwszych postaci drgań zawierających zarówno mody giętne oraz skrętne, jak i jedną modę wzdłużną. Do oceny wpływu elementów aktywnych na uzyskane postacie drgań badanej belki wykorzystano kryterium dopasowania modalnego (ang. Modal Assurance Criterion, MAC). Zaprezentowana praca stanowi wstępny etap badań, których celem jest wyznaczenie optymalnego położenia elementów aktywnych sterujących dynamiką łopat wirnika śmigłowca.